Original Research Paper

IJES *Iranian Journal of Earth Sciences*
Vol. 15, No. 3, 2023, 155-162.
DOI: 10.30495/ijes.2022.1955008.1734

An interpretation of airborne magnetic data to characterize Nickel-Copper mineralization over Mpemba Hill, Blantyre Malawi

Joshua Chisambi*[1], Tiyamike Haundi[1]

1. Department of Mining Engineering, Malawi University of Business and Applied Sciences, Blantyre, Malawi.

Received 3 March 2022; accepted 16 July 2022

Abstract

The present study seeks to characterize Ni-Cu mineralization at Mpemba hill in Blantyre, southern Malawi by using aeromagnetic and drill hole data. The area has been under-explored for this im-portant economic commodity and as such not much is known regarding its mineralization poten-tial. The minimal curvature gridding technique was utilised to grid the aeromagnetic data, and a grid cell size of 50 m was employed. The Ni-Cu host lithologies are characterized by high mag-netism, and are mostly ultramafic rocks. Drilling results indicates that the mineralization starts at depths from 50m and remains open. The area is associated with disseminated and blebby type of mineralization and the mineralization is associated with high magnetic signatures in ultramafic meta pyroxenite bodies yielding high base metal values. Euler model depths analysis of the mag-netic sources is deep, lies at 3.2 km depth and the shallower magnetic bodies lie between 100 m and 1km. The depth estimates show that the mineralization is near surface and goes deep, so fur-ther exploration should not be limited to shallow depth. The ultramafic rocks are potential sites for Ni-Cu mineralization in the area and Mpemba hill has a huge potential to find economic min-eralization suitable for mining.

Keywords: *Geophysical Survey, Disseminated sulphides, Nickel- Copper, Drilling, Ore type, Mpemba.*

1. Introduction

Geophysical exploration has played a vital role in mineral exploration. In Malawi, with the vast land and the rapid development of the economy, ground-based geophysical exploration is getting more and more difficult to meet the requirements of mineral exploration for its low efficiency and limited access caused by inaccessible terrain. Airborne geophysical exploration has become an important tool to quickly investigate large-scale subsurface with lower time and economic costs in remote, uninhabitable areas. Airborne magnetics survey is one of the most widely used airborne geophysical explorations, especially in mineral exploration. This exploration method plays an important role in greenfield exploration for many types of deposits because of its ability to map bedrock geology in a self-consistent fashion and, most importantly, through the cover.

Such data are particularly useful for identifying geological environments favorable for the formation of Cu-Ni deposits as these deposits are often associated with changes in the amounts of magnetic minerals, such as magnetite and pyrrhotite, in the host rocks. Magmatic sulfide deposits of Ni, Cu, Co, and the platinum group elements (PGEs) are usually associated with mafic or ultramafic magmatism derived from the mantle (Hutchins and Reeves 1980 ,Fichler et al. 1999, Evans et al. 2000, Barnes et al. 2016,). For the study of regional magmatism and the identification of Ni-Cu deposits, detailed studies based on geophysical data are important (Hutchins and Reeves 1980, Evans et al. 2000, Chernicoff et al. 2002, e.g Aitken and Betts 2009, Li et al. 2015, Barnes et al. 2016 and 2019, Kohanpour et al. 2018, Diakov et al. 2019, Ge et al. 2020).

Magnetic anomalies characterize the magmatic systems associated with these deposits and associated rocks (mafic-ultramafic complexes) and may be detected by magnetic data (Fichler et al. 1999).

Malawi hosts numerous mineral occurrences such as Ni-Cu, gold base metals and PGEs, yet detailed information regarding the mode of mineralization remains scanty in the published literature. A conspicuous paucity in Nickel resources in Malawi's mineral inventory may be partially attributed to a general low resolution in the knowledge of Malawi's geology, coupled with historical under-exploration for this important economic commodity. Neighboring countries Mozambique, Zambia, and Tanzania have abundant mineral resources, yet comparatively little is known about Malawi, despite these countries occurring in the same tectonic zone as Malawi and sharing similarities in their geological histories.

One area in which Ni-Cu mineralization has been discovered in Malawi is Mpemba in Blantyre. The Ni-Cu endowment of this area remains relatively under-studied and is thus poorly constrained.

The Malawi Agenda 2063 has prioritized mining as one of the pillars that can help to improve the country's ailing economy. In a bid to achieve this, the Malawi Government has recently conducted an airborne magnetic survey covering the whole country to uncover her true mineral potential. The newly acquired aeromagnetic data are utilized in this paper to assess the mineral potential of Mpemba area, southern Malawi by exploring and delineating mafic-ultramafic complexes associated with Ni-Cu sulfide mineralization. The study concentrates on

----

*Corresponding author.
E-mail address (es): jjchisambi@gmail.com

the possibility of economic nickel-copper mineral deposits at Mpemba area, which is believed to be a promising target for prospecting activities. This study will be very important to Malawi Government and mineral exploration companies interested to invest in Malawi as it presents insight regarding nickel-copper mineralization in the study area.

2. Geological Setting

The Mpemba prospect is located in southern Malawi, 20 kilometers southwest of Blantyre. It consists of a succession of pyroxenitic to gabbroic intrusive rocks with widespread nickel sulfide disseminations and clots, as well as a Ni and Cu soil geochemical anomaly spanning over 3km^2 (Bloomfield and Garson 1965).
The granulite facies meta igneous rocks dominate the Mpemba region. The Ni-Cu sulfides are found in the Mpemba Hill pyroxenite body, and there is a variety of granitic to syenitic intrusions in the surrounding country rocks, all of which are mild to severely impacted by penetrative deformation (Bloomfield and Garson 1965). These have a close spatial and perhaps chronological connection with ultramafic rocks on a regional scale. Banded biotite-amphibole-garnet gneisses, felsic to intermediate migmatites, and minor amphibolite gneisses are the main lithologies around the Mpemba Hill intrusion (Fig 1). The Mpemba Hill pyroxenite formation, as well as numerous smaller satellite intrusive structures nearby, contain Ni-Cu sulfide mineralization. The Mpemba Hill body is lensoidal (5 x 2 km at the surface) and concentrically zoned, with gneissic gabbronorite at the edges, fine to medium-grained feldspathic pyroxenite outer core, and coarse, granular pyroxenite in the center (Fig 1), (Evans 2011). Websterite is the most common ultramafic lithology, consisting primarily of green augite and a small amount of hypersthene, with biotite, hornblende, and plagioclase as minor constituents (British Geological Survey 2009; Yazdi et al. 2015). A crystallographically controlled exsolution network of red-brown spinel or opaque oxide is found in both hypersthene and augite, while green hercynitic spinel is present in accessory quantities interstitially to the pyroxenes (British Geological Survey 2009).

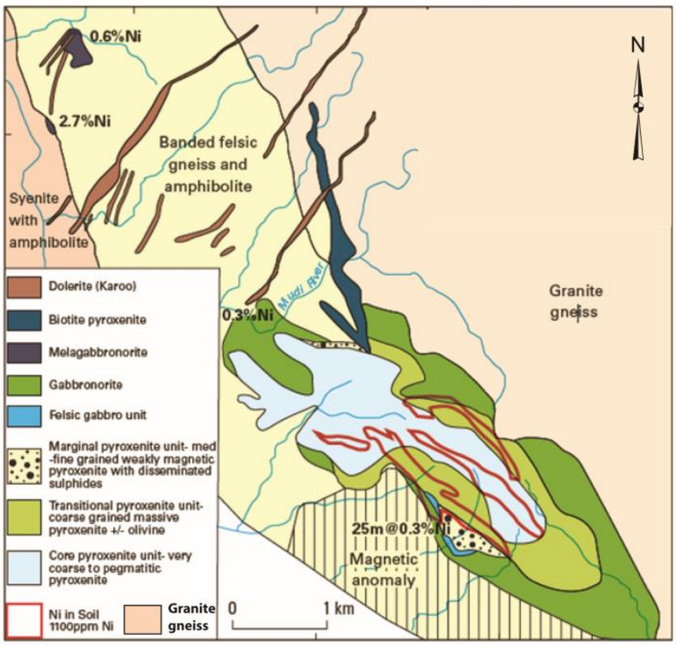

Fig 1. Geological map of the study area (modified from British Geological Survey 2009)

3. Methods

3.1. Airborne Geophysics

A high-resolution geophysical survey was carried out between 2013 and 2014 by Sander Geophysics Limited (SGL) under the auspices of the World Bank's Mining Governance and Growth Support Project (MGGSP) in Malawi. Airborne geophysical data were collected over the entire country using Scintrex Cesium vapour magnetometers installed on a Cessna Caravan fixed-wing airplane which was flying at an altitude of 80 meters terrain clearance and line spacing of 250 meters apart. The flight line had a NE-SW orientation and tie line spacing of 2000 meters. The WGS 84 Datum and Universal Transverse Mercator (UTM) map projection were used in the data processing. The survey included observations of magnetic anomalies and gamma-ray spectrometric measurements(Sander Geophysics 2013; Jafari and Yazdi 2014). Transient magnetic variation effects were corrected and the International Geomagnetic Reference Field (IGRF 2005 model) was eliminated from the magnetic data. This IGRF corrected aeromagnetic anomaly data is the basis for all subsequent interpretations. Later, Geosoft Oasis Montaj software was used to process all geophysical data (Geosoft 2008). Specifically, minimal curvature gridding technique, with a 50 m grid cell size was used to grid the original data lines (Briggs 1974).

Because the Earth's magnetic field fluctuates at the location of measurement, magnetic anomalies usually have complex shapes. In order to fix this, the total magnetic field was reduced the pole (Kis 1990, Büyüksaraç et al. 2005, Ates et al. 2008, Ateş et al. 2009 , Rozimant et al. 2009, Ates et al. 2012, Ekinci et al. 2020). This reduction positions the anomalies more directly over their causative bodies, and hence makes interpretation easier (Li 2008). The resulting grids were further filtered to enhance any high-intensity magnetic bodies and structures. The filters that were applied include the upward continuation, first vertical derivative (Cooper and Liu 2011), and tilt derivative (MacLeod and Jones 1993). The upward continuation filter was used to delineate the edges of the deep magnetic anomalies. Linear geological features such as faults, dykes were enhanced by tilt and first vertical derivatives and these derivatives provided an excellent base for structural interpretation (AlSaud 2008). The processed images were then used to extract geological features by visual image interpretation (Drury 2001).

Euler deconvolution technique was used to provide depth estimate to magnetic sources over the study area. This approach delineates the geometry of magnetic bodies using structural indices (SI) and is based on Euler homogeneous equation (Aziz et al 2013)

$$(x-x_0)\frac{\partial T}{\partial x}+(y-y_0)\frac{\partial T}{\partial y}+(z-z_0)\frac{\partial T}{\partial z}=N(B-T) \qquad (1)$$

where (x0,y0,z0) is the location of a magnetic source whose total field is observed at (x,y,z), $\frac{\partial T}{\partial x}\frac{\partial T}{\partial y}$ and $\frac{\partial T}{\partial z}$ are derivatives of the magnetic field in the x, y, and z respectively while B is the value of the regional value of the total field. The homogeneity degree N is construed as a structural index (Reid et al 1990).

The structural index SI defines the anomaly attenuation rate at the observation point and depends on the nature of the field source. The RTP aeromagnetic data were used for calculation of the Euler's deconvolution solutions using structural indices (SI) of 0, 0.5, 1, 2, and 3 and a window size of 10 × 10 m. "a window size of 10 × 10 m" means a squared window with a dimension of 10*50 m=500m (10×cell size). To remove the short-wavelength cultural noise without significantly smoothing the data, the aeromagnetic data was upward continued to an elevation of 150 m before computing the Euler deconvolution.

3.2 Drilling and samples and test

Drilling was done in all areas with high magnetic signatures in order to intercept the magnetic anomalies at depth. Drilled lithological units within these high magnetic zones were sampled for subsequent mineralogical analyses.

The goal of the sampling was to investigate the geochemistry of the units to identify geochemical fingerprints that indicate mineralization. Mineralogical analyses were conducted at the ALS mineral services laboratory (Johannesburg, South Africa) using WD-XRF. All of the core samples were sliced in half, washed, and dried. Half of each sample was crushed and pulverized in an agate mill to produce a powder with a particle size of less than 75 µm.

4. Results and Discussion

4.1. Total magnetic intensity map (TMI)

Aeromagnetic data are commonly used to investigate the earth's geological features, and they may help with both understanding hidden geological formations and mineral prospecting (Chisambi et al. 2021). The aeromagnetic data from Mpemba metallogenic belt is shown in Fig 2 and it reveals a considerable wide variation in the values of magnetic intensity ranging from_259.3 to -193.1 nT. These differences are caused by lithologic or topographic alterations. They are represented by a changing color spectrum, with the magnetic high (Red) indicating the presence of mafic rocks and the low (Blue) indicating the presence of less ferromagnetic materials. The center and eastern portions of the map is characterized by positive magnetic anomaly, features, whereas the northwestern portion has magnetic low features. The study region's highest amplitude value is 259.3 nT, which is related to meta pyroxenite and metagabro. The magnetic highs are circular to ellipsoidal in shape, with a diameter of 5-10 km and a length of 30-40 km, and they are SE-trending.

Magmatic sulfide deposits of Ni, Cu, Co and the platinum group elements (PGE) are usually associated with mafic or ultramafic magmatism and portray high magnetic affinities.

We infer that the host rock to the Ni-Cu sulfide mineralization at Mpemba is this high magnetic ultramafic meta pyroxenite. It can be clearly identified by the aeromagnetic data and it is primarily made up of pyroxenite and meta pyroxenite, with lesser amounts of olivine orthopyroxenite, peridotite, minor websterite, and gabbroic rocks with granoblastic to poikilitic textures in some places. The rock is locally altered and metamorphosed to amphibolite and host extensively amphibolitized schistose equivalents in enveloping high-strain zones. It is pervasively mineralized with disseminated, minor net-textured, through to localized semi-massive vein sulfide mineralization.

On the other hand, the minimum amplitude value is about -193.05 nT. associated with basement gneissic rocks. The magnetic lows in the northwestern part reflect non-mineralized basement gneisses. Longer spatial wavelength magnetic anomalies are likely related to the Mpemba pluton that intruded these basement gneisses. The map of aeromagnetic data upward continued to 5 km (Fig 2b) highlights the anomalies with longer spatial wavelengths.

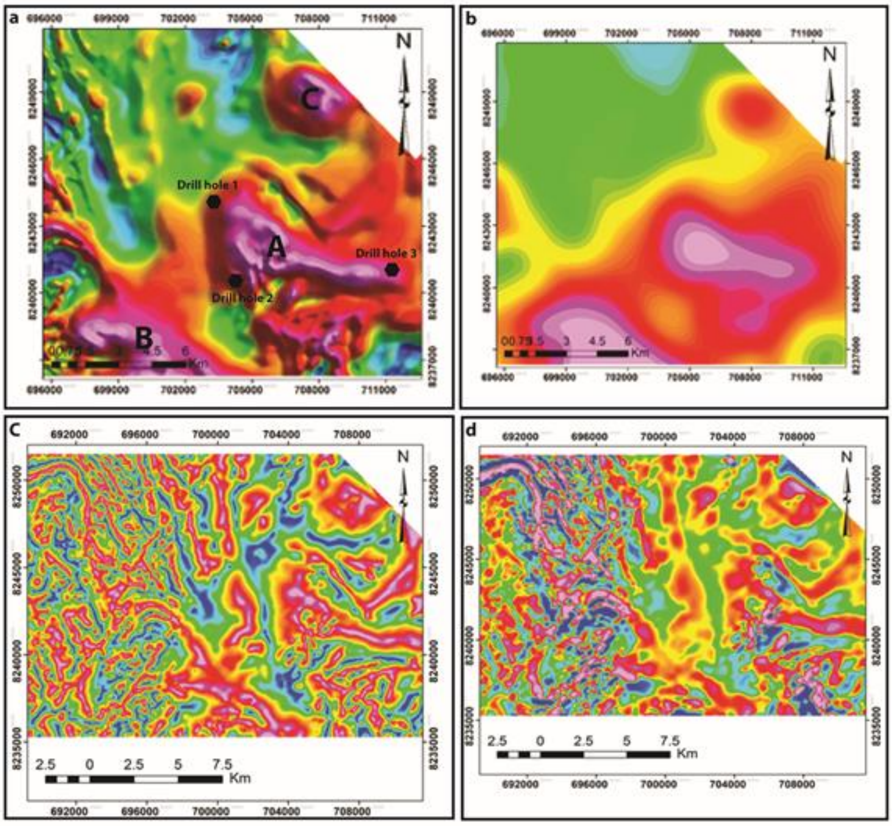

Figure 2. (a) Total Magnetic map of the study area reduced to pole indicating areas of high mag-netic intensity associated with mineralization. (b) Upward continued total magnetic map (c and d)Tilt Derivative and Vertical Derivative maps indicating dyke swarms that trend in the NW-SE direction. These were the conduit for magma emplacement in the study area.

Applying an upward continuation filter (Fig2b) shows that the central and southern parts are characterized by these high magnetic anomalies. The upward continuation filter accentuates deep anomalies and removes the shallow ones. Therefore, these anomalies are from deep sources and are probably related to the magmatic activity. The southeastern section of the map has moderate and broad anomalies, which are caused by thick intrusive rocks (meta pyroxenites). Upward continuation, filtered most aeromagnetic anomalies with shorter spatial wavelengths associated with shallow igneous rocks.

Fig 2c and d. are the tilt and vertical derivative images of the study area. The area is characterized by linear features trending NW-SE. These features are dyke swarms that characterize the study area. The tilt and vertical derivative map clearly show the response of the dykes as short-wavelength linear anomalies that crosscut the study area. The present study allows the mapping of these numerous dykes that were formerly un-known because they were either hidden by cover or did not reach the surface. These dyke swarms acted as conduits for magma emplacement. Furthermore, the aeromagnetic data is characterized by NW-SE-trending major crustal and secondary faults. The delineated high magnetic zones in Total and Upward continued map (A, B and C) are located near the faults and display similar NW- SE-trending axes, suggesting that these faults are possible passageways for the rapid uprising of magma for these high magnetic zones (ore body complexes?). Fig 3 shows the radial averaged spectrum of the aeromagnetic data of study area and the depth estimate of its analysis. It shows that the wave number is between 0 and 10 km^{-1}. The depth to the magnetic sources estimated based on the slope of the energy spectrum shows magnetic depths that correspond with 1–3 km.

From the Euler solutions, it can be seen that the model depths of the magnetic sources are deep, lies at 3.2 km depth and the shallower magnetic bodies lie between 100 m and 1000 m (Fig 4). These depth estimates correlate very well with those obtained using spectral analysis and shows that the mineralization is near surface and goes deep, so further exploration should not be limited to shallow depth.

The observed magnetic anomalies (A, B and C) in the Total Magnetic and upward continued maps show one broad elongated anomaly which implies that the source body is located at a relatively large depth.

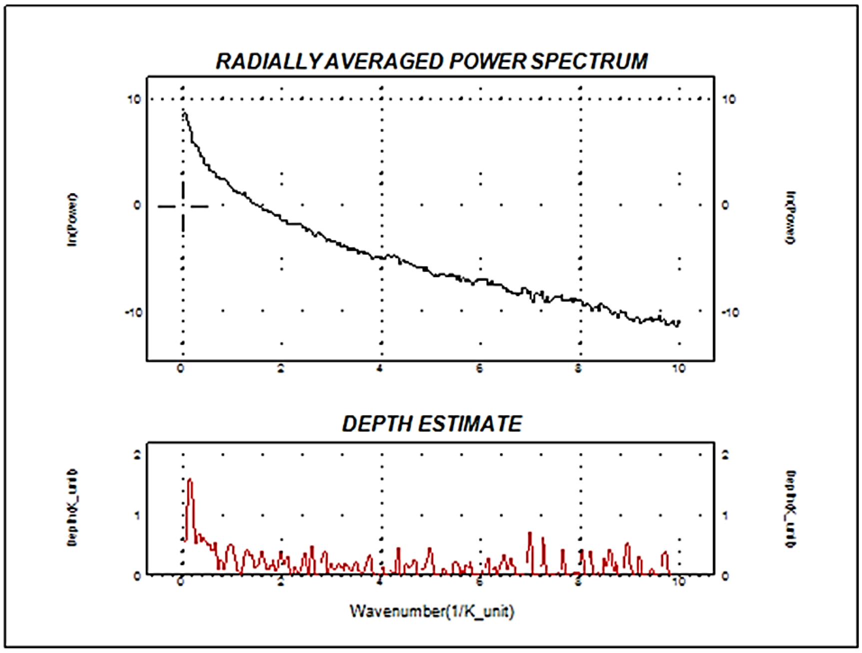

Fig 3. Radially averaged power spectrum indicating depth of the sources

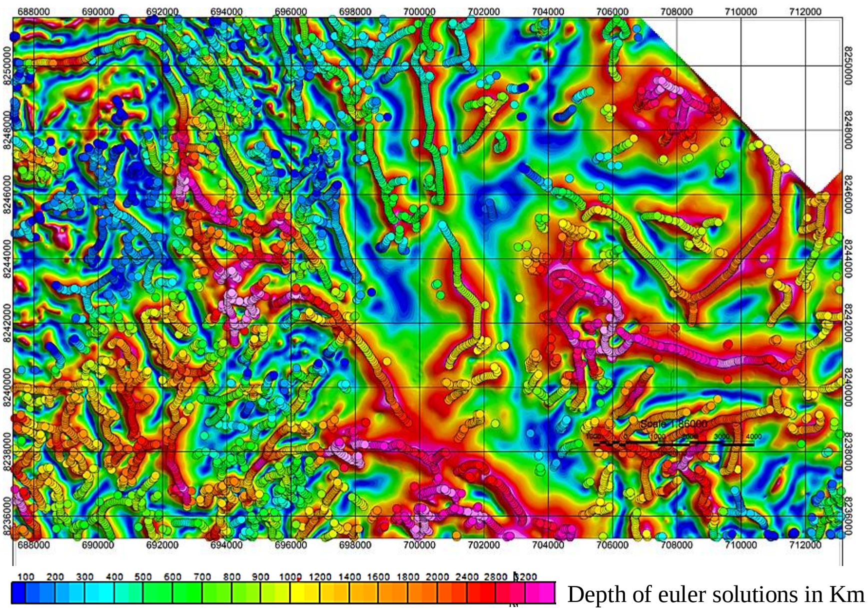

Fig 4. Euler solutions overlain on the Tilt derivative map

4.2. Geological interpretation of drill hole data

The Ni-Cu ore bodies are characterized by high magnetism, and occur mostly in ultramafic rocks. Therefore, the ultramafic rocks are potential areas for Ni-Cu mineralization in Malawi.

Based on the geophysical signatures described above, the high-positive magnetic anomalies associated with the magnetite-enriched zones (A, B, C) are related to igneous rock with higher mafic contents and the nickel mineralization and provide a larger exploration target for nickel-copper mineralized zones. As such these zones should be delineated for further exploration work.

We drilled in the high magnetic zone A (Fig 2a) to see if we can intercept mineralization. Three 200 m diamond drill holes were drilled, and all the holes were associated with sulfide mineralization confirming the presence of mineralization (Fig 5). The discovery of these high magnetic meta-igneous rocks in the Mpemba area, via geophysics and their confirmation by geological field work provides us with new ideas about the nickel mineralisation potential in the study area.

This exploration drilling effort aimed to check if we can intercept mineralization and possibly assess the scale of the mineralization. Drilling indicates near-surface mineralization distributed over a wide area.

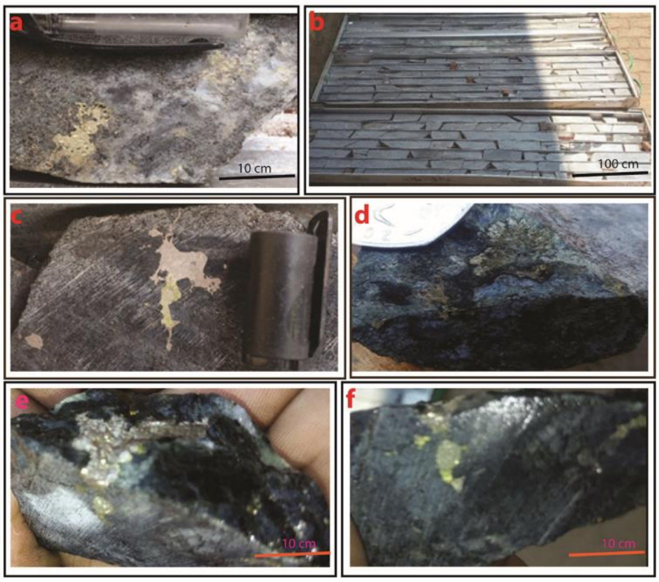

Fig 5. (a-f) Sections of drill cores drilled in the study area indicating the ore minerals found in the area and blebby sulfide type of mineralization

Fig 6.(a-c). Disseminated sulfide type of mineralization

All the 3 holes drilled intersect near-surface mineralization starting from 50m depth and the mineralization still remains open. The intersection of sulfide-hosted mineralization indicates the potential for identification of a significant body of mineralization at depth.

Pyrrhotite, pentlandite, chalcopyrite, and pyrite are the main ore minerals found in the Mpemba ultramafic meta pyroxenite intrusion (Figures 5and 6). The main sulfide mineral in the ore is pyrrhotite.

4.3. Ore Type

There are two kinds of mineralization at Mpemba: (1) A blebby pyrite-chalcopyrite assemblage (Fig 5); and (2) A disseminated chalcopyrite-pyrite assemblage (Fig 6)

4.3.1 Blebby sulfides Style of mineralization

This mineralization type is the most conspicuous, with irregular sulfide blebs up to 2 cm in diameter strewn around the meta pyroxenites. The blebs are mostly composed of pyrite (70%) with some chalcopyrite (30%) as a sequence of cross-cutting veins/slivers, solitary inclusions, and rims around the margins of the pyrite (Fig 5).

4.3.2 Disseminated sulfides

The bulk of the mineralization takes the form of disseminated interstitial sulfide blebs primarily in the 0.2- to 8-mm size range within dominantly pyroxenitic rocks (Fig 6). Disseminated, where sulfides, together with other interstitial minerals, are disseminated between olivine grains and are not interconnected. In general, disseminated sulfides represent between 1 and 35 mol.% of the rock. The sulfide generally appears as isolated spots in the silicate rocks.

4.4. Mineralogical analyses Assay results

Assay results of 3 reconnaissance drill holes at Mpemba Hill (Zone A, in Table 1) confirm the presence of widespread mineralization. Drill core rock samples yield assay results of up to 2.9% Ni and 1.6 % Cu, along strike to the northwest of the main intrusion. This indicates that the area has a high potential to find economic Nickel mineralization and further detailed exploration work is recommended.

Table 1. Assay results for selected samples

Sample	Ni	Cu
	%	%
BH2/35	2.9	1.6
BH3/70	1.31	0.55
BH1/60	1.14	0.36

5. Conclusion

In this study, we have provided the first insights regarding nickel mineralization following a reconnaissance exploration that was undertaken at Mpemba hill in Malawi to possible exploration companies interested in investing in Malawi. We have interpreted newly airborne magnetic data in relation to mineral exploration for nickel. The Ni-Cu host lithologies are characterized by high magnetism, and are mostly ultramafic rocks. As such, the ultramafic rocks in the area are probable sites for Ni-Cu mineralization. According to this study, potential positions for Ni-Cu mineralization in Mpemba has been defined. Three areas, which are respectively marked as A, B, and C, deserve further prospecting. Drilling results in area A indicate that the bore hole intersected with ultramafic rocks, and mineralization starts at depths from 50m. The Mpemba area is associated with disseminated and blebby type of mineralization. The area has a huge potential to find economic mineralization which can lead to mining. Mineralization is associated with high magnetic signatures in ultramafic meta pyroxenite bodies yielding high base metal values. This indicates that the area has a high prospect to find economic nickel mineralization and further detailed exploration work is recommended. The discovery of these high magnetic meta-igneous rocks in the Mpemba area, via geophysics and their confirmation by geological field work provides us with new ideas about the nickel mineralisation potential in the study area, leading to new genetic concept for Nickel mineralization. Use of modern geophysical software such as Geosoft allowed a better visualisation and improved interpretation of geophysical data and, in this way, lead to better understanding of aeromagnetic anomalies.

References

Aitken ARA, Betts PG (2009) Multi-scale integrated structural and aeromagnetic analysis to guide tectonic models: An example from the eastern Musgrave Province, Central Australia, *Tectonophysics* 476(3–4): 418–435.

AlSaud MM (2008) Structural mapping from high resolution aeromagnetic data in west central Arabian Shield, Saudi Arabia using normalized derivatives, *Arabian Journal of Geosciences* 1(2): 129–136.

Ates A, Bilim F, Buyuksarac A, Bektas Ö (2008) A tectonic interpretation of the Marmara Sea, NW Turkey from geophysical data. *Earth, Planets and Space* 60(3): 169–177.

Ates A, Bilim F, Buyuksarac A, Aydemir A, Bektas O, Aslan Y (2012) Crustal Structure of Turkey from Aeromagnetic, Gravity and Deep Seismic Reflection Data, *Surveys in Geophysics* 33(5): 869–885.

Ateş A, Büyüksaraç A, Bilim F, Bektaş Ö, Şendur Ç, Komanovali G (2009) Spatial correlation of the aeromagnetic anomalies and seismogenic faults in the Marmara region, NW Turkey, *Tectonophysics* 478(1–2): 135–142.

Aziz AM, Sauck WA, Shendi EA, Rashed MA, Abd El-Maksoud M (2013) Application of Analytic Signal and Euler Deconvolution in Archaeo-Magnetic Prospection for Buried Ruins at the Ancient City of Pelusium, NW Sinai, Egypt: A Case Study, *Surveys in Geophysics* 34(4): 395–411.

Barnes SJ, Cruden AR, Arndt N, Saumur BM (2016) The mineral system approach applied to magmatic Ni–Cu–PGE sulphide deposits, *Ore Geology Reviews* 76: 296–316.

Barnes SJ, Mole DR, Hornsey R, Schoneveld LE (2019) Nickel-copper sulfide mineralization in the Ntaka Hill ultramafic complex, Nachingwea region, *Tanzania. Economic Geology* 114(6): 1135–1158.

Bloomfield K, Garson MS (1965) The Geology of the Kirk Range-Lisungwe Valley Area. Ministry of Natural Resources, Geological Survey Department. Bulletin No.17. The Government Printer, Zomba. Malawi.

Briggs I (1974) Machine Contouring Using Minimum Curvature, *Geophysics* 39(1):39-48

British Geological Survey. (2009). Mineral potential of Malawi (Issue January).

Büyüksaraç A, Jordanova D, Ateş A, Karloukovski V (2005) Interpretation of the gravity and magnetic anomalies of the Cappadocia region, Central Turkey, *Pure and Applied Geophysics* 162(11): 2197–2213.

Chernicoff CJ, Richards JP, Zappettini EO (2002) Crustal lineament control on magmatism and mineralization in northwestern Argentina: Geological, geophysical, and remote sensing evidence, *Ore Geology Reviews* 21(3–4): 127–155.

Chisambi J, Haundi T, Tsokonombwe G (2021) Geologic structures associated with gold mineralization in the Kirk Range area in Southern Malawi, *Open Geosciences* 13(1): 1345–1357.

Cooper SM, Liu T (2011) Journal of African Earth Sciences A magnetic and gravity investigation of the Liberia Basin, West Africa, *Journal of African Earth Sciences* 59(2–3): 159–167.

Diakov S, West R, Schissel D, Krivtsov A, Kochnev-Pervoukhov V, Migachev I (2019) Recent Advances in the Noril'sk Model and Its Application for Exploration of Ni-Cu-PGE Sulfide Deposits.

Drury S (2001) Image interpretation in geology. Blackwell science; Nelson Thornes.

Ekinci YL, Büyüksaraç A, Bektaş Ö, Ertekin C (2020) Geophysical Investigation of Mount Nemrut Stratovolcano (Bitlis, Eastern Turkey) Through Aeromagnetic Anomaly Analyses, *Pure and Applied Geophysics* 177(7): 3243–3264.

Evans DM (2011) Geodynamic setting of Neoproterozoic nickel sulphide deposits in eastern Africa, *Applied Earth Science* 120(4):175–186.

Evans DM, Boadi I, Byemelwa L, Gilligan J, Kabete J, Marcet P, Sy A (2000) Kabanga Magmatic Nickel Sulphide Deposits, Tanzania:Morphology and Geochemistry of Associated Intrusions, *Journal of African Earth Sciences* 1;30(3):651-74.

Fichler C, Rundhovde E, Olesen O, Sæther BM, Rueslåtten H, Lundin E, Doré AG (1999) Regional tectonic interpretation of image enhanced gravity and magnetic data covering the mid-Norwegian shelf and adjacent mainland, *Tectonophysics* 306(2): 183–197.

Ge T, Qiu L, He J, Fan Z, Huang X, Xiong S (2020) Aeromagnetic identification and modeling of mafic-ultramafic complexes in the Huangshan-Turaergen Ni-Cu metallogenic belt in NW China: Magmatic and metallogenic implications, *Ore Geology Reviews* 127: 103849.

Geophysics S (2013) Data Processing Report High Resolution Airborne Magnetic and Gravity Survey : The Comprehensive Countrywide Airborne Geophysical Survey for The Government of The Republic of Malawi , The Ministry of Mining.

Geosoft (2008) Oasis montaj Viewer 7.0 The core software platform for working with large volume spatial data quick starttm tutorial.

Hutchins DG, Reeve, CV (1980) Regional Geophysical Exploration of the Kalahari in Botswana, *Tectonophysics* 69: 201–220.

Jafari HR, Yazdi A (2014) Radioactive Anomalies in 1: 50000 Dehbakri Sheet, South of Kerman Province, Iran, *Open Journal of Geology*, 04(08): 399-405.

Kis KI (1990) Transfer properties of the reduction of magnetic anomalies to the pole and to the equator, *Society of Exploration Geophysics* 55(9): 1141–1147.

Kohanpour F, Lindsay MD, Occhipinti S, Gorczyk W (2018) Structural controls on proterozoic nickel and gold mineral systems identified from geodynamic modelling and geophysical interpretation, east Kimberley, Western Australia, *Ore Geology Reviews* 95: 552–568.

Li C, Zhang Z, Li W, Wang Y, Sun T, Ripley EM (2015) Geochronology, petrology and Hf-S isotope geochemistry of the newly-discovered Xiarihamu magmatic Ni-Cu sulfide deposit in the Qinghai-Tibet plateau, western China, *Lithos* 1;216: 224-40.

Li X (2008) Magnetic reduction-to-the-pole at low latitudes: Observations and considerations, *The Leading Edge* 27(8): 990–1002.

MacLeod IN, Jones K., Dai TF (1993) 3-D Analytic signal in the interpretation of total magnetic field data at low magnetic latitudes. Explo-annotated, *Exploration Geophysics* 993;24(4): 679-88

Reid AB, Allsop JM, Granser H, Millett AJ, Somerton IW (1990) Magnetic interpretation i n three dimensions using Euler deconvolution, *Geophysics* 55(1): 80-91.

Rozimant K, Büyüksaraç A, Bektaş Ö (2009) Interpretation of magnetic anomalies and estimation of depth of magnetic crust in Slovakia, *Pure and Applied Geophysics* 166: 471-84.

Yazdi A, Ziaaldini S, Dabiri R (2015) Investigation on the Geochemical Distribution of REE and Heavy Metals in Western Part of Jalal-Abad Iron Ore Deposit, Zarand, SE of Iran, *Open Journal of Ecology* 5 (09): 460-476.